Tissue Engineering

DOI: 10.1089/ten.TEA.2016.0510

Physioxia promotes the articular chondrocyte-like phenotype in human chondroprogenitor-derived self-organized tissue

Devon E. Anderson, PhD[1] Brandon D. Markway, PhD,[1] Kenneth Weekes, BS,[1] Helen McCarthy, PhD,[2] Brian Johnstone, PhD[1]

[1]Oregon Health & Science University

Department of Orthopaedics & Rehabilitation

3181 SW Sam Jackson Park Road, OP31

Portland, OR 97239

[2]Cardiff University
School of Biosciences
Sir Martin Evans Building
Cardiff, Wales, United Kingdom CF10 3AX

Abstract:

Introduction: Biomaterial-based tissue engineering has not successfully reproduced the structural architecture or functional mechanical properties of native articular cartilage. In scaffold-free tissue engineering systems, cells secrete and organize the entire extracellular matrix over time in response to environmental signals, such as oxygen level. In this study, we investigated the effect of oxygen on the formation of neocartilage from human-derived chondrogenic cells.

Methods: Articular chondrocytes (ACs) and articular cartilage progenitor cells (ACPs) derived from healthy human adults were guided toward cell condensation by centrifugation onto plate inserts that were uncoated or coated with either agarose or fibronectin. Neocartilage discs were cultured at hyperoxic (20%) or physioxic (5%) oxygen levels, and biochemical, biomechanical and molecular analyses were used to compare the cartilage produced by ACs versus ACPs.

Results: Fibronectin-coated inserts proved optimal for growing cartilaginous discs from both cell types. In comparison with culture in hyperoxia, AC neocartilage cultured at physioxia exhibited a significant increase in chondrogenic gene expression, proteoglycan production, and mechanical properties with a concomitant decrease in collagen content. At both oxygen levels, ACP-derived neocartilage produced tissue with significantly enhanced mechanical properties and collagen content relative to AC-derived neocartilage. Both ACs and ACPs produced substantial collagen II and reduced levels of collagens I and X in physioxia relative to hyperoxia. Neocartilage from ACPs exhibited anisotropic organization characteristic of native cartilage with respect to collagen VI of the pericellular matrix when compared with AC-derived neocartilage; however, only ACs produced abundant surface-localized lubricin.

Discussion & Conclusions: Guiding human-derived cells toward condensation and subsequent culture in physioxia promoted the articular cartilage tissue phenotype for ACs and ACPs. Unlike ACs, ACPs are clonable and highly expandable while retaining chondrogenicity. The ability to generate large tissues utilizing a scaffold-free approach from a single autologous progenitor cell may represent a promising source of neocartilage destined for cartilage repair.

Introduction:

Cartilage pathologies are the most common cause of chronic disability among adults in the United States, and early intervention to repair focal defects is key to restoring tissue integrity before chronic degeneration (1-3). Unfortunately, successful surgical repair remains a challenge as the resultant tissues are usually fibrocartilaginous and cannot meet the functional demands of the joint (4). The limited long-term success of current strategies suggests a need for tissue engineering approaches to recapitulate the structural and biomechanical properties of articular cartilage.

In cartilage tissue engineering, biomaterials are used to provide initial structure; however, the resultant tissue phenotype is constrained by biomaterial influences (5). Over the past decade, a number of scaffold-free methods have emerged: self-assembled tissues, which form through cell interaction and condensation in the absence of external stimuli (6-11), and self-organizing models relying on external cues to guide the cells toward condensation. For the latter, cells are typically centrifuged and/or cultured onto substrates such as porous polymer (12-17) or protein-coated membranes (18-21). One goal of the current work was to develop a reliable and repeatable method to produce large-scale scaffold-free neocartilage constructs. To this end, we hypothesized that fibronectin, which is the earliest extracellular matrix protein produced following cell condensation (22,23), would provide necessary cues to drive cell condensation toward a defined geometry during *in vitro* tissue culture.

The selection of a cell type with high chondrogenic and anabolic capacities is essential to generate scaffold-free cartilage. Stem and progenitor cell populations mitigate the challenges of availability of primary chondrocytes and their phenotypic modulation during expansion. Articular cartilage progenitor cells (ACPs) are postulated to reside in the upper zone of adult cartilage after forming the tissue through appositional growth (24-27). They can be clonally expanded *in vitro* and maintain differentiation potential following extended population doublings with minimal differentiation toward hypertrophy compared with mesenchymal stem cells (MSCs) (28,29). To date, tissue engineering utilizing human ACPs is limited to scaffold-based systems (30,31).

While cells within a scaffold-free tissue will determine tissue phenotype, the culture environment will guide tissue development. Without a blood supply, native articular chondrocytes have a physioxia ranging from 1 to 5% oxygen (8-40 mmHg) (32,33). We have previously shown that lowering oxygen from hyperoxia (20% O_2) to physioxia significantly enhances chondrogenesis of expanded human chondrocytes (34). We have more recently discovered that the responses to altered oxygen tension for both MSCs and ACPs are dependent on the intrinsic chondrogenicity of

the cells, and physioxia drives differentiation toward the stable phenotype for highly chondrogenic cells (35). Thus, we sought to develop scaffold-free neocartilage from adult human cells in physioxia with optimization of medium volume and cell density to maintain tissue viability. The ACP clones used were chosen from those characterized in our prior work as highly chondrogenic (35). We hypothesized that in comparison with heterogeneous ACs, clonal ACPs would generate tissue closer to the articular cartilage phenotype, and that lowered oxygen tension would facilitate its extracellular matrix maturation.

Materials & Methods:

Cell Isolation: Normal human femoral condyles were obtained postmortem (n = 5 for AC, n = 3 for ACP) with Institutional Review Board approval at Oregon Health & Science University (Portland, OR, USA) and the NHS Blood and Tissue bank (Liverpool, UK). Full thickness human articular cartilage was dissected, minced and digested as described previously (35). Following digestion, ACs were expanded in low glucose DMEM, 10% (v/v) fetal bovine serum (FBS) and 1% (v/v) P/S. ACPs were isolated from separate donor tissue in the same manner as ACs through sequential pronase (70 U/ml for 20 min at 37°C) and type I collagenase (300 U/ml for 4 hr at 37°C) digestion. Directly following cell isolation from tissue, ACPs were selected from the total chondrocyte population through differential adhesion to fibronectin (27), and clonal populations were isolated with cloning rings. Colonies were expanded in monolayer in low glucose DMEM/F12 (1:1), 10mM HEPES, 10% (v/v) FBS, 1% (v/v) P/S, 0.1 mM ascorbic acid 2-phosphate (Wako, Cape Charles, VA), 1 ng/ml transforming growth factor β1 (TGF-β1, PeproTech, Rocky Hill, NJ, USA) and 5 ng/ml FGF-2 (PeproTech). ACs and ACPs were plated at 1 x 10^6 cells and expanded in atmospheric oxygen and 5% CO_2 through two passages. At final cell harvest, ACPs had undergone 22-24 population doublings from a single cell origin and ACs had undergone 4 population doublings from a heterogeneous population.

Tissue Culture: Both ACs and ACPs were passaged with TrypLE reagent (Life Technologies) and resuspended at a density of 2 x 10^6 cells per 200 µl in serum-free chondrogenic differentiation medium (36). Cell density was selected based on initial experiments with 1, 1.5, 2, or 3 x 10^6 cells per tissue; whereby, 2 x 10^6 of each cell type reliably produced a tissue of maximum thickness; void tissue cores developed at higher cell seeding densities. Cell suspensions were pipetted into Transwell inserts (6.5 mm diameter, 0.4 µm pore size, polyester; Corning, Inc., Corning, NY, USA), either uncoated, coated with 2% agarose (w/v), or coated with 50 µg/ml fibronectin (CalBioChem, Merck, Darmstadt, Germany). The cell-laden inserts were centrifuged at 200 × g for 5 min in 24-well plates with 1 ml medium below the membrane. Two days later, the inserts were suspended in 12-well plates containing 4.8 ml medium and cultured on an orbital shaker at 1 Hz frequency at 5% oxygen (physioxia) or at 20% oxygen (hyperoxia), and 5% CO_2. Medium was changed twice weekly, with physioxia maintained in a low oxygen chamber (BioSpherix, Lacona, NY, USA) with pre-gassed medium. After ten days, tissues were released from the membrane into free swelling culture in 0.9% w/v poly-2-hydroxyethylmethacrylate (poly-HEMA) (Sigma-Aldrich, St. Louis, MO, USA)

coated 12-well plates containing 3 ml differentiation medium, a minimum volume optimized for high cell densities based on our prior work. Cultures were maintained for 28 days with the originally membrane-oriented side facing upward.

Biochemical Analysis: Triplicate samples from each condition were weighed, rinsed with phosphate-buffered saline (PBS), and digested overnight at 60°C in 4 U/ml papain (Sigma-Aldrich) in PBS containing 6 mM Na_2-ethylenediaminetetraacetic acid and 6 mM L-cysteine (papain buffer, pH 6.0). Total DNA and sulfated glycosaminoglycan (GAG) content were quantified using Hoechst dye and 1,9-dimethymethylene blue (DMMB) assays, respectively, as described previously (34). Hydroxyproline content was quantified using an adaptation of the chloramine-T hydrate oxidation/p-dimethylaminobenzaldehyde method as described previously (34).

Biomechanical Analysis: Mechanical properties of three replicates from each condition were tested in unconfined compression (37). Sample dimensions were measured with a digital micrometer, and the tissue subjected to a creep test under 0.02 N load until equilibrium was reached at ~300 s. Upon equilibrium, iterative stress relaxation tests were performed at 1 mm/s to 10, 20, 30, and 40% compressive strain to derive the equilibrium compressive Young's modulus at each ramp. Between each stress relaxation ramp, a dynamic test was carried out by applying 1% oscillatory strain at 1 Hz frequency to derive the dynamic modulus.

Gene Expression Analysis: RNA was isolated from three biological replicates in each condition. Tissues were pooled, snap frozen, crushed and lysed with buffer RLT (QIAGEN, Germantown, MD, USA) containing 40mM dithiothreitol (DTT). RNA isolation was performed with the RNeasy Mini Kit (QIAGEN) and reverse-transcribed using qScript cDNA SuperMix (Quanta BioSciences, Gaithersburg, MD, USA). Quantitative polymerase chain reaction was performed with cDNA using a StepOnePlus thermal cycler (Life Technologies, Grand Island, NY, USA) with TaqMan Fast Advanced Master Mix and primers (supplemental table 1) according to previously reported parameters (35).

Histology and Immunohistochemistry: Tissue from each condition was formalin-fixed, paraffin-embedded (FFPE) and sectioned or frozen in cold boiling hexanes, mounted in OCT and sectioned. Toluidine blue (0.04% in 0.2M acetate buffer, pH 4.0) was applied to visualize proteoglycans. FFPE sections were deparaffinized, and frozen sections were fixed in 4% PFA at 4°C for 10 min, prior to antigen retrieval. For collagens I and II, pretreatment of FFPE sections with 1 mg/ml protease (Roche) in 1X PBS for 30 min at room temperature was followed by 0.1% (w/v) hyaluronidase (Sigma-Aldrich) in 1X PBS for 45 min at 37°C. FFPE sections were pretreated with protease only for collagen X and frozen sections were pretreated with hyaluronidase only for perlecan. For lubricin and collagen VI, FFPE sections were pretreated in pre-heated citrate buffer (10mM sodium citrate, 0.05% Tween-20, pH 6.0) for 5 min at 55°C and 550 Watts in a BioWave microwave (Ted Pella, Redding, CA) followed by 0.1% hyaluronidase for 45 min at 37°C. All sections were blocked with 5% bovine serum albumin (BSA) in 1X PBS, and incubated overnight at 4°C with primary antibodies to collagen I (1:200; kind gift from A Hollander, University of Bristol, Bristol, UK), collagen II (1:200; II-II6B3, Developmental Studies Hybridoma Bank, University of Iowa, Iowa City, IA, USA), collagen X (1:300; kind gift from GJ Gibson, Henry Ford Hospital, Detroit, MI, USA), perlecan (1:200; MAB1948P, Merck Millipore, Darmstadt, Germany), lubricin (1:200; MABT401, Merck Millipore) or collagen VI (1:200; sc-20649, Santa Cruz Biotechnologies, Dallas, TX, USA). Sections were washed with PBS and incubated for 45 min at room temperature with Oregon Green-conjugated goat anti-rabbit (1:250) or Alexa Fluor 596-conjugated goat anti-mouse (1:250) (Life Technologies), diluted in 1% BSA in 1X PBS. Slides were mounted with ProLong Gold containing 4',6-diamidino-2-phenylindole (DAPI, Life Technologies).

Collagen Protein Analysis: Enzyme-linked immunosorbent assays (ELISA) were used to quantify collagens I and II. Discs were flash frozen, pulverized and lyophilized then assayed according to manufacturer instructions (Chondrex, catalog #6018, #6021).

Statistical Analysis: Three biological replicates were used for each ACP experiment (n=3), five biological replicates were used for each AC experiment (n=5), and three technical

replicates were used for each analytical method. Normality for each condition among each cell type was assessed using a D'Agostino-Pearson omnibus K2 test, with normally distributed groups not meeting significance of $p<0.05$ for distribution other than Gaussian. Comparison of biochemical parameters and gene expression between physioxia and hyperoxia within a given group was assessed using a paired t-test for normal data and Wilcoxon matched-pairs signed rank test for non-normal data, with significance set at $p<0.05$. Comparison between normally distributed data of each cell type was performed with an unpaired t-test, with significance set at $p<0.05$. Mean and standard deviation for fold-change gene expression was calculated as physioxia relative to hyperoxia for each group.

Results:

Fibronectin directs tissue geometry in scaffold-free constructs. Both ACs and ACPs formed flat discs of a defined geometry over 28 days of culture in a self-organization system through centrifugation, cell condensation on a fibronectin-coated membrane, and extracellular matrix elaboration (Figure 1). In contrast, both cell types contracted into large pellets within 24 hours of culture in inserts coated with 2% agarose indicating that an adherent substrate was necessary to define tissue geometry in early scaffold-free constructs (Figure 2). In agreement with prior work (18), ACs retained a flat disc morphology on uncoated porous polyester membranes yet consistently lacked proteoglycans throughout the tissue depth. ACPs, however, contracted into large pellets within 24 hours. When cultured on a fibronectin-coated porous polyester membrane, both cell types reliably formed a flat disc with proteoglycans produced throughout the depth (Figure 2). As a primary objective of the study was to create tissues of a flattened and uniform disc shape, only tissues generated in fibronectin-coated Transwell inserts were used for the remainder of the experiments.

Physioxia promotes biochemical anabolism of ACs. Compared with culture in hyperoxia, ACs in physioxia produced significantly more total GAGs; however, this increase was not significant when normalized to DNA content (Figure 3). In contrast, ACPs did not produce significantly more GAGs in physioxia versus hyperoxia but produced significantly more GAGs than ACs in hyperoxia, a difference retained with normalization to DNA. DNA content was not different between cell types or oxygen levels. There was no statistically significant difference in total collagen for either cell type between oxygen levels, but ACP-derived neocartilage contained significantly more collagen in physioxia compared with AC-derived neocartilage. There were no differences in wet weight or thickness between cell types or oxygen levels.

Physioxia enhances the bulk mechanical properties of AC neocartilage, but ACP neocartilage is mechanically superior. AC-derived neocartilage cultured at physioxia had significantly higher compressive equilibrium modulus for stress relaxation tests at 10 and 20% strain than in hyperoxia (Figure 4). It also exhibited strain stiffening behavior—increasing in stiffness with increasing deformational compressive strain. The compressive equilibrium modulus for ACP-derived neocartilage was not different in physioxia versus hyperoxia but was significantly higher than that for AC-derived neocartilage at matched oxygen level for each strain ramp, and with strain stiffening behavior in physioxia. The dynamic modulus for 1% dynamic strain at 1Hz frequency was not different between cell types or oxygen levels.

Physioxia promotes the stable articular chondrocyte phenotype. Relative to culture in hyperoxia, ACs in physioxia had a significant fold-change increase in expression of many genes associated with the articular phenotype (*COL2A1*, *COL11A2*, *COL9A1*, *ACAN*, *SOX9*, *PRG4*) and a significant decrease in genes of the fibrocartilaginous (*COL1A1*) and hypertrophic (*MMP13*) phenotypes (Figure 5). *COL10A1* was also consistently decreased among replicates, but not to a significant level. There was no difference between the gene expression profile for ACPs cultured in hyperoxia versus physioxia although *COL2A1*, *COL1A1* and *COL10A1* were each changed in the same direction but to a smaller magnitude. Genes coding for *SOX9* and *L-SOX5* were decreased in ACPs. Regardless of oxygen tension, *COL2A1*, *ACAN* and *COL1A1* were highly expressed for both ACs and ACPs relative to the housekeeping gene; *PRG4* was highly expressed for ACs, but very low for ACPs.

Physioxia promotes articular cartilage matrix protein production. ACP and AC-derived neocartilage had similar proteoglycan and collagen II distributions (Figure 6A). Collagen I was present throughout the matrix after 28 days of culture in hyperoxia but more localized to the outer edges in physioxia for both cell types. Collagen X was detectable for AC-derived neocartilage cultured in hyperoxia but undetectable at physioxia. In contrast it was undetectable in all ACP-derived neocartilage regardless of oxygen tension. ACPs expressed more collagen II than I protein and expressed significantly less collagen I than ACs, even though ACs had an improved II:I ratio in physioxia (Figure 6B). AC-derived neocartilage produced lubricin that was primarily localized to the side contacting the well that was agitated during culture. This expression was independent of oxygen tension (Figure 7). In contrast, lubricin was not detectable in ACP-derived neocartilage. Investigation of pericellular proteins revealed that perlecan was distributed throughout the bulk of matrix for both cell types while collagen VI was more pericellular for only ACPs; both protein distributions were independent of oxygen level.

Discussion:

Expanded adult human chondrocytes contracted into pellets in non-adherent culture but produced a disc-like tissue morphology when cultured on a polymer substrate, consistent with a previous report (21). However, ACPs needed a fibronectin substrate initially. Fibronectin is the earliest expressed extracellular matrix molecule during cell condensation (22,23), and this, plus the high binding affinity between fibronectin and ACPs during their isolation, informed our decision to employ fibronectin as opposed to other matrix molecules previously used to guide scaffold-free self-organization (21). The ability to define tissue morphology in a scaffold-free approach will ultimately be necessary to develop personalized therapies for focal cartilage defect repair. To this end, other groups have recently developed sophisticated molds to guide cell condensation into large-scale cartilaginous tissues (17,38). As a foundation for ACPs as a novel cell type in scaffold-free tissue engineering, we found that these cells generated uniform discs when simply cultured on fibronectin-coated membranes.

This is the first report of scaffold-free tissue engineering utilizing ACPs. Few studies have extensively investigated scaffold-free tissue engineering from adult human-derived cells; the only study to directly compare scaffold-free tissues generated from adult human chondrocytes and MSCs used a single biologic donor for each (39). Studies of scalable scaffold-free techniques indicate that neonatal mammalian primary chondrocytes build tissues with characteristics of articular cartilage following self-assembly (6,9) or self-organization (18). However, it was not clear whether these were viable strategies to generate tissues with adult human-derived cells, which are limited in metabolism and expansion potential in comparison with neonatal or juvenile mammalian cells (40,41).

One study suggested that low oxygen is detrimental to the development of scaffold-free neocartilage (20) but we posit that the central voids found were the result of tissue anoxia from nutrient deprivation, previously characterized by both diffusion modeling and oxygen delivery experiments (42,43). We generated tissues without a central void through optimization of cell seeding density and medium volume. In accordance with our previous data from re-differentiating expanded human chondrocytes in pellet culture (34,35), physioxia promoted the stable chondrocyte phenotype in scaffold-free discs. Lowering oxygen stabilizes hypoxia-inducible factors (HIFs), which are targeted for proteosomal degradation in the presence of oxygen. HIFs, in turn, regulate genes with hypoxia responsive elements (HRE), drive chondrogenesis toward the articular chondrocyte phenotype, and modulate extracellular matrix metabolism (44). In physioxia, ACs

significantly upregulated genes with HREs, including *SOX9* and *PRG4*, which also led to a downstream increase in SOX-9 targets—*COL2A1* and *ACAN*. Although all ACP clones upregulated *COL2A1* in physioxia, the response was not statistically significant. We have previously shown that the response of postnatal human stem cells to lowered oxygen depends on the intrinsic chondrogenic differentiation capacity, and highly chondrogenic ACP clones were less responsive at the gene level than poorly chondrogenic clones. We therefore did not expect significant differences in ACP gene expression based on our prior results with these same cells in pellet culture (35). The only significant difference in gene expression between hyperoxia versus physioxia for ACPs was decreased *SOX9*, possibly a consequence of examining gene expression after 28 days of culture—a time point much later than the induction of differentiation by TGF-ß and physioxia when *SOX9* is promoted. Both cell types consistently downregulated *COL10A1* of the hypertrophic chondrocyte phenotype, and ACs significantly downregulated *COL1A1* and *MMP13*; results consistent with our previous work exploring the role of physioxia in regulating hypertrophy (34,35). However, it is important to point out that ACP expression of these genes/proteins is minimal even in hyperoxia for the highly chondrogenic clones selected for this work, based on our prior studies (35).

Culture in physioxia significantly increased the bulk equilibrium modulus for AC-derived neocartilage, concomitant with increased total GAG production. Consistent with our prior results (35), the highly chondrogenic ACP clones used in this study were less responsive to lowered oxygen tension with respect to GAG synthesis in comparison with ACs. These cells, however, produced significantly more GAGs in hyperoxia than ACs and had likely reached a maximum rate of proteoglycan synthesis regardless of oxygen tension. While compressive stiffness directly correlates with proteoglycan content in native tissue (45), a >10-fold higher equilibrium modulus of ACP- relative to AC-derived tissue was not attributable only to proteoglycan content based on equivalent GAG levels in physioxia. These differences in compressive stiffness that are not attributable to proteoglycan content likely involve other constituents of the extracellular matrix, including collagen. There were not only differences in the total collagen content but also in the collagen types between AC- and ACP-derived tissues, with more collagen II in ACP-derived neocartilage. Increased collagen may be complemented by greater collagen crosslinking in physioxia through lysyl oxidase, which has an HRE, to drive a further increase in compressive modulus similar to mechanisms of postnatal native tissue maturation (46). Previous studies have shown that lowered oxygen increases collagen crosslinking in scaffold-free tissues generated from primary bovine chondrocytes (8). In physioxia, both AC- and ACP-derived neocartilage exhibited

strain stiffening behavior—a property of the collagen network of mature articular cartilage that immature postnatal tissues lack (46); and possibly due to enhanced collagen crosslinking. Unlike the compressive equilibrium modulus, the dynamic modulus was not different between tissue types or oxygen level. In native tissue, dynamic modulus is proportional to collagen content (45); however, ACP-derived neocartilage did not have a significantly higher dynamic modulus despite increased collagen content in physioxia. This may be a consequence of the relatively low total collagen content and dynamic stiffness in all neocartilage discs in comparison with native tissues.

Further investigation of the extracellular matrix revealed that the collagen expression profile was improved with culture in physioxia relative to hyperoxia for neocartilage from both ACs and ACPs—maintaining global collagen II expression but apparently decreasing collagen I and X throughout the tissues. These results are consistent with those for pellet culture of each cell type (34,35). In comparison with ACPs, ACs produced significantly more collagen I in hyperoxia; results that are consistent with known collagen profiles following expansion and dedifferentiation of chondrogenic cells (47,48). Consistent with gene expression data, ACs responded favorably to lowered oxygen with a reduction in collagen I toward the level of ACPs, resulting in an increase in the ratio of collagen II to collagen I more similar to the phenotype of native articular cartilage. Regardless of oxygen tension, AC-derived neocartilage did not show evidence of pericellular matrix localization of collagen VI or perlecan, with these proteins expressed throughout the bulk of the matrix. In contrast, ACP-derived neocartilage had collagen VI localized to the pericellular matrix after 28 days. Since these proteins are distributed throughout the matrix in neonatal cartilage and subsequently localized to the pericellular matrix with maturation (49,50), this result suggests greater matrix maturity for ACP-derived neocartilage.

Independent of oxygen level, ACs produced lubricin, localized primarily to one surface of the disc. In contrast, ACPs did not produce detectible amounts of lubricin. Chondroprogenitors have recently been identified by *PRG4* expression (26) or lubricin production (51,52) *in vivo*, but this is the first study to investigate lubricin and *PRG4* expression during *in vitro* differentiation of ACPs. Lack of *PRG4* and lubricin expression may indicate that these cells are subject to phenotypic modification when isolated, cloned, expanded and/or differentiated *in vitro*. Alternatively, ACPs may represent a progenitor population up- or down-stream from the *PRG4*-expressing lineage identified *in vivo* (26,53), or the cell populations may be entirely distinct; these remain future topics for investigation.

Our results indicate that physioxic culture is beneficial for neocartilage development toward the articular cartilage phenotype. Highly chondrogenic ACPs clones produced a tissue that was mechanically superior and more mature than tissues derived from ACs. Unlike ACs, ACP discs were derived from a single cell following clonal isolation and expansion. The ability to produce large-scale scaffold-free constructs of a defined geometry from this adult human cell source may eventually allow us to generate tissues that satisfy the structural and functional demands required for articular cartilage repair, and thus be able to offer personalized and autologous therapies for focal articular cartilage injuries.

Author's Contributions:

DA contributed to study conception, experimental design, cell and tissue culture, biochemical analyses, statistical analyses, and manuscript preparation. BM contributed to study conception, experimental design, and manuscript revision. KW contributed to histological analyses and manuscript revision. HM contributed to cell and tissue culture and manuscript revision. BJ contributed to study conception, experimental design, result analyses, and manuscript revision. All authors have read and approved the manuscript.

Acknowledgements:

The authors thank the following surgeons for providing human tissue: Dr. Dennis Crawford at Oregon Health and Science University (OHSU) and Dr. Paul Rooney at the NHS Blood and Tissue bank (Liverpool, UK) for providing healthy human articular cartilage. We would like to thank Ms. Teresa Pizzuto at Case Western Reserve University for technical assistance in histologic specimen processing. Finally, we would like to thank Dr. Robert Mauck and Breanna Seiber at the University of Pennsylvania for providing tools and assistance in characterization of the mechanical properties of neocartilage. This work was supported by funding from NIH/NIAMS (1R21AR064431) and the OHSU Foundation.

References:

1. Murphy L, Schwartz TA, Helmick CG, Renner JB, Tudor G, Koch G, et al. Lifetime risk of symptomatic knee osteoarthritis. Arthritis Rheum. **59**(9), 1207, 2008.

2. Murphy LB, Helmick CG, Schwartz TA, Renner JB, Tudor G, Koch GG, et al. One in four people may develop symptomatic hip osteoarthritis in his or her lifetime. Osteoarthr Cartilage. Elsevier Ltd; **18**(11), 1372, 2010.

3. McCormick F, Harris JD, Abrams GD, Frank R, Gupta A, Hussey K, et al. Trends in the Surgical Treatment of Articular Cartilage Lesions in the United States: An Analysis of a Large Private-Payer Database Over a Period of 8 Years. Arthroscopy. Arthroscopy Association of North America; **30**(2), 222, 2014.

4. Makris EA, Gomoll AH, Malizos KN, Hu JC, Athanasiou KA. Repair and tissue engineering techniques for articular cartilage. Nat Rev Rheumatol. Nature Publishing Group; **11**(1), 21, 2014.

5. Athanasiou KA, Eswaramoorthy R, Hadidi P, Hu JC. Self-Organization and the Self-Assembling Process in Tissue Engineering. Annu Rev Biomed Eng. **15**(1), 115, 2013.

6. Hu JC, Athanasiou KA. A Self-Assembling Process in Articular Cartilage Tissue Engineering. Tissue Eng. **12**(4), 1, 2006.

7. Ofek G, Revell CM, Hu JC, Allison DD, Grande-Allen KJ, Athanasiou KA. Matrix Development in Self-Assembly of Articular Cartilage. Koutsopoulos S, editor. PLoS ONE. **3**(7), e2795, 2008.

8. Makris EA, Hu JC, Athanasiou KA. Hypoxia-induced collagen crosslinking as a mechanism for enhancing mechanical properties of engineered articular cartilage. Osteoarthr Cartilage. Elsevier Ltd; **21**(4), 634, 2013.

9. Novotny JE, Turka CM, Jeong C, Wheaton AJ, Li C, Presedo A, et al. Biomechanical and Magnetic Resonance Characteristics ofa Cartilage-like Equivalent Generated in a Suspension Culture. Tissue Eng. **12**(10), 2755, 2006.

10. Kraft JJ, Jeong C, Novotny JE, Seacrist T, Chan G, Domzalski M, et al. Effects of Hydrostatic Loading on a Self-Aggregating, Suspension Culture-Derived Cartilage Tissue Analog. Cartilage. **2**(3), 254, 2011.

11. Mohanraj B, Farran AJ, Mauck RL, Dodge GR. Time-dependent functional maturation of scaffold-free cartilage tissue analogs. J Biomech. Elsevier; **47**(9), 2137, 2014.

12. Naumann A, Dennis JE, Aigner J, Coticchia J, Arnold J, Berghaus A, et al. Tissue Engineering of Autologous Cartilage Grafts in Three- Dimensional in vitro Macroaggregate Culture System. Tissue Eng. **10**(11/12), 1695, 2004.

13. Murdoch AD, Grady LM, Ablett MP, Katopodi T, Meadows RS, Hardingham TE. Chondrogenic Differentiation of Human Bone Marrow Stem Cells in Transwell Cultures: Generation of Scaffold-Free Cartilage. Stem Cells. **25**(11), 2786, 2007.

14. Elder SH, Cooley AJ, Borazjani A, Sowell BL, To H, Tran SC. Production of Hyaline-like Cartilage by Bone Marrow Mesenchymal Stem Cells in a Self-Assembly Model. Tissue Eng Pt A. **15**, 3025, 2009.

15. Mayer-Wagner S, Schiergens TS, Sievers B, Docheva D, Betz OB, Jansson V, et al. Membrane-Based Cultures Generate Scaffold-Free Neocartilage In Vitro: Influence of Growth Factors. Tissue Eng Pt A. **16**(2), 513, 2010.

16. Whitney GA, Mera H, Weidenbecher M, Awadallah A, Mansour JM, Dennis JE. Methods for Producing Scaffold-Free Engineered Cartilage Sheets from Auricular and Articular Chondrocyte Cell Sources and Attachment to Porous Tantalum. BioResearch. **1**(4), 157, 2012.

17. Bhumiratana S, Eton RE, Oungoulian SR, Wan LQ, Ateshian GA, Vunjak-Novakovic G. Large, stratified, and mechanically functional human cartilage grown in vitro by mesenchymal condensation. PNAS. 2014.

18. Hayes AJ, Hall A, Brown L, Tubo R, Caterson B. Macromolecular Organization and In Vitro Growth Characteristics of Scaffold-free Neocartilage Grafts. J Histochem Cytochem. **55**(8), 853, 2007.

19. Lee WD, Hurtig MB, Kandel RA, Stanford WL. Membrane Culture of Bone Marrow Stromal Cells Yields Better Tissue Than Pellet Culture for Engineering Cartilage-Bone Substitute Biphasic Constructs in a Two-Step Process. Tissue Eng Pt C Met. **17**(9), 939, 2011.

20. Qu C, Lindeberg H, Ylärinne JH, Lammi MJ. Five percent oxygen tension is not beneficial for

neocartilage formation in scaffold-free cell cultures. Cell Tissue Res. **348**(1), 109, 2012.

21. Rutgers M, Saris DB, Vonk LA, van Rijen MH, Akrum V, Langeveld D, et al. Effect of Collagen Type I or Type II on Chondrogenesis by Cultured Human Articular Chondrocytes. Tissue Eng Pt A. **19**(1-2), 59, 2013.

22. Singh P, Schwarzbauer JE. Fibronectin and stem cell differentiation - lessons from chondrogenesis. J Cell Sci. **125**(16), 3703, 2012.

23. Singh P, Schwarzbauer JE. Fibronectin matrix assembly is essential for cell condensation during chondrogenesis. J Cell Sci. **127**(20), 4420, 2014.

24. Hayes AJ, MacPherson S, Morrison H, Dowthwaite GP, Archer CW. The development of articular cartilage: evidence for an appositional growth mechanism. Anat Embryol. **203**, 469, 2001.

25. Dowthwaite GP, Bishop JC, Redman SN, Khan IM, Rooney P, Evans DJR, et al. The surface of articular cartilage contains a progenitor cell population. J Cell Sci. **117**(6), 889, 2004.

26. Kozhemyakina E, Zhang M, Ionescu A, Ayturk UM, Ono N, Kobayashi A, et al. Identification of a Prg4-Expressing Articular Cartilage Progenitor Cell Population in Mice. Arthritis Rheum. **67**(5), 1261, 2015.

27. Williams R, Khan IM, Richardson K, Nelson L, McCarthy HE, Analbelsi T, et al. Identification and Clonal Characterisation of a Progenitor Cell Sub-Population in Normal Human Articular Cartilage. Agarwal S, editor. PLoS ONE. **5**(10), e13246, 2010.

28. Khan IM, Bishop JC, Gilbert S, Archer CW. Clonal chondroprogenitors maintain telomerase activity and Sox9 expression during extended monolayer culture and retain chondrogenic potential. Osteoarthr Cartilage. Elsevier Ltd; **17**(4), 518, 2009.

29. McCarthy HE, Bara JJ, Brakspear K, Singhrao SK, Archer CW. The comparison of equine articular cartilage progenitor cells and bone marrow-derived stromal cells as potential cell sources for cartilage repair in the horse. Vet J. Elsevier Ltd; **192**(3), 345, 2012.

30. Neumann AJ, Alini M, Archer CW, Stoddart MJ. Chondrogenesis of Human Bone Marrow-Derived Mesenchymal Stem Cells Is Modulated by Complex Mechanical Stimulation and Adenoviral-Mediated Overexpression of Bone Morphogenetic Protein 2. Tissue Eng Pt A.

19(11-12), 1285, 2013.

31. Frisbie DD, McCarthy HE, Archer CW, Barrett MF, McIlwraith CW. Evaluation of Articular Cartilage Progenitor Cells for the Repair of Articular Defects in an Equine Model. J Bone Joint Surg. **97**(6), 484, 2015.

32. Carreau A, Hafny-Rahbi BE, Matejuk A, Grillon C, Kieda C. Why is the partial oxygen pressure of human tissues a crucial parameter? Small molecules and hypoxia. J Cell Mol Med. **15**(6), 1239, 2011.

33. Lund-Olesen K. Oxygen tension in synovial fluids. Arthritis Rheum. **13**(6), 769, 1970.

34. Markway BD, Cho H, Johnstone B. Hypoxia promotes redifferentiation and suppressesmarkers of hypertrophy and degeneration in bothhealthy and osteoarthritic chondrocytes. Arthritis Res Ther. BioMed Central Ltd; **15**(4), R92, 2013.

35. Anderson DE, Markway BD, Bond D, McCarthy HE, Johnstone B. Responses to altered oxygen tension are distinct between human stem cells of high and low chondrogenic capacity. Stem Cell Res Ther. Stem Cell Research & Therapy; 1, 2016.

36. Johnstone B, Hering T, Caplan AI, Goldberg VM, Yoo JU. In vitro chondrogenesis of bone marrow-derived mesenchymal progenitor cells. Exp Cell Res. **238**, 265, 1998.

37. Mauck R, Yuan X, TUAN R. Chondrogenic differentiation and functional maturation of bovine mesenchymal stem cells in long-term agarose culture. Osteoarthr Cartilage. **14**(2), 179, 2006.

38. Bhumiratana S, Vunjak-Novakovic G. Engineering physiologically stiff and stratified human cartilage by fusing condensed mesenchymal stem cells. Methods. Elsevier Inc; 1, 2015.

39. Murphy MK, Huey DJ, Hu JC, Athanasiou KA. TGF-β1, GDF-5, and BMP-2 Stimulation Induces Chondrogenesis in Expanded Human Articular Chondrocytes and Marrow-Derived Stromal Cells. Stem Cells. **33**(3), 762, 2015.

40. Wilson B, Novakofski KD, Donocoff RS, Liang YXA, Fortier LA. Telomerase Activity in Articular Chondrocytes Is Lost after Puberty. Cartilage. SAGE Publications; **5**(4), 215, 2014.

41. Barbero A, Grogan S, Schäfer D, Heberer M, Mainil-Varlet P, Martin I. Age related changes in

human articular chondrocyte yield, proliferation and post-expansion chondrogenic capacity. Osteoarthr Cartilage. **12**(6), 476, 2004.

42. Armstrong JPK, Shakur R, Horne JP, Dickinson SC, Armstrong CT, Lau K, et al. Artificial membrane-binding proteins stimulate oxygenation of stem cells during engineering of large cartilage tissue. Nat Commun. Nature Publishing Group; **6**, 1, 2016.

43. Zhou S, Cui Z, Urban JPG. Factors influencing the oxygen concentration gradient from the synovial surface of articular cartilage to the cartilage-bone interface: A modeling study. Arthritis Rheum. **50**(12), 3915, 2004.

44. Murphy CL, Thomas BL, Vaghjiani RJ, Lafont JE. HIF-mediated articular chondrocyte function: prospects for cartilage repair. Arthritis Res Ther. **11**(213), 1, 2009.

45. Van C Mow, Gu WY, Chen FH. Structure and Function of Articular Cartilage and Meniscus. In: Mow VC, Huiskes R, editors. Basic Orthopaedic Biomechanics & Mechano-biology. 3rd ed. Philadelphia: Lippincott Williams & Wilkins; p. 181–258, 2005.

46. Gannon AR, Nagel T, Bell AP, Avery NC, Kelly DJ. Postnatal changes to the mechanical properties of articular cartilage are driven by the evolution of its collagen network. Eur Cells Mater. **29**, 105, 2015.

47. Goessler UR, Bugert P, Bieback K, Baisch A, Sadick H, Verse T, et al. Expression of collagen and fiber-associated proteins in human septal cartilage during in vitro dedifferentiation. Int J Mol Med. **14**(6), 1015, 2004.

48. Goessler UR, Bieback K, Bugert P, Naim R, Schafer C, Sadick H, et al. Human chondrocytes differentially express matrix modulators during in vitro expansion for tissue engineering. Int J Mol Med. **16**(4), 509, 2005.

49. Kvist AJ, Nyström A, Hultenby K, Sasaki T, Talts JF, Aspberg A. The major basement membrane components localize to the chondrocyte pericellular matrix — A cartilage basement membrane equivalent? Matrix Biol. **27**(1), 22, 2008.

50. Zhang Z. Chondrons and the Pericellular Matrix of Chondrocytes. Tissue Engineering Part B: Reviews. **21**(3), 267, 2015.

51. Seol D, McCabe DJ, Choe H, Zheng H, Yu Y, Jang K, et al. Chondrogenic progenitor cells

respond to cartilage injury. Arthritis Rheum. **64**(11), 3626, 2012.

52. Zhou C, Zheng H, Seol D, Yu Y, Martin JA. Gene expression profiles reveal that chondrogenic progenitor cells and synovial cells are closely related. J Orthop Res. **32**(8), 981, 2014.

53. Lefebvre V, Bhattaram P. Editorial: Prg4-Expressing Cells: Articular Stem Cells or Differentiated Progeny in the Articular Chondrocyte Lineage? Arthritis Rheum. **67**(5), 1151, 2015.

54. Park S, Hung CT, Ateshian GA. Mechanical response of bovine articular cartilage under dynamic unconfined compression loading at physiological stress levels. Osteoarthr Cartilage. **12**(1), 65, 2004.

55. Mansour JM. Biomechanics of Cartilage. In: Oatis CA, editor. Kinesiology: the mechanics and pathomechanics of human movement. Lippincott, Williams & Wilkens; p. 66–79, 2003.

Corresponding Author:

Devon E Anderson, PhD.

Department of Orthopaedics & Rehabilitation

Oregon Health & Science University

3181 SW Sam Jackson Park Rd, HRC529C

Portland, OR 97239

FIGURE LEGEND:

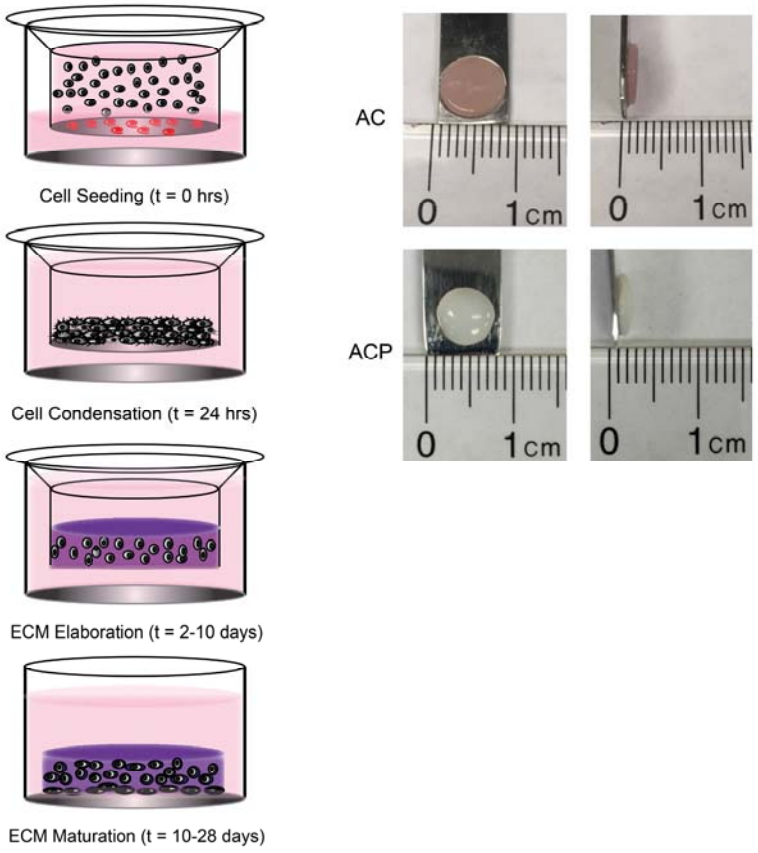

Figure 1. (A) Schematic representing stages of self-organization of scaffold-free neocartilage beginning with cell seeding via centrifugation onto a protein-coated membrane to direct cell condensation into a restricted geometry. Over the course of culture, cells produce an extracellular matrix that starts as an immature homogenous matrix and matures over time with signals from the culture environment. (B) Gross images of AC and ACP-derived neocartilage show that each cell type produced a disc of uniform dimensions after 28 days of culture.

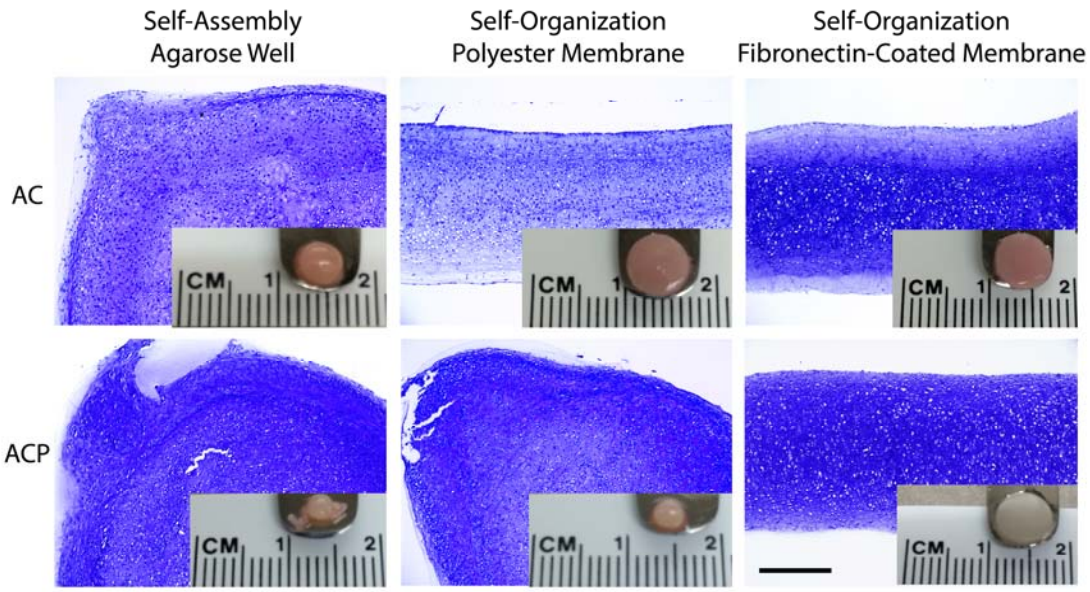

Figure 2. Toluidine blue histology and gross images demonstrate that human-derived ACs and ACPs formed a large pellet when cultured in non-adherent agarose wells after seeding into a flattened disc. Only ACs retained a disc morphology when cultured on porous polyester membranes, but both cell types retained a disc morphology when cultured on a polyester membrane coated with fibronectin. Scale bars = 400 µm.

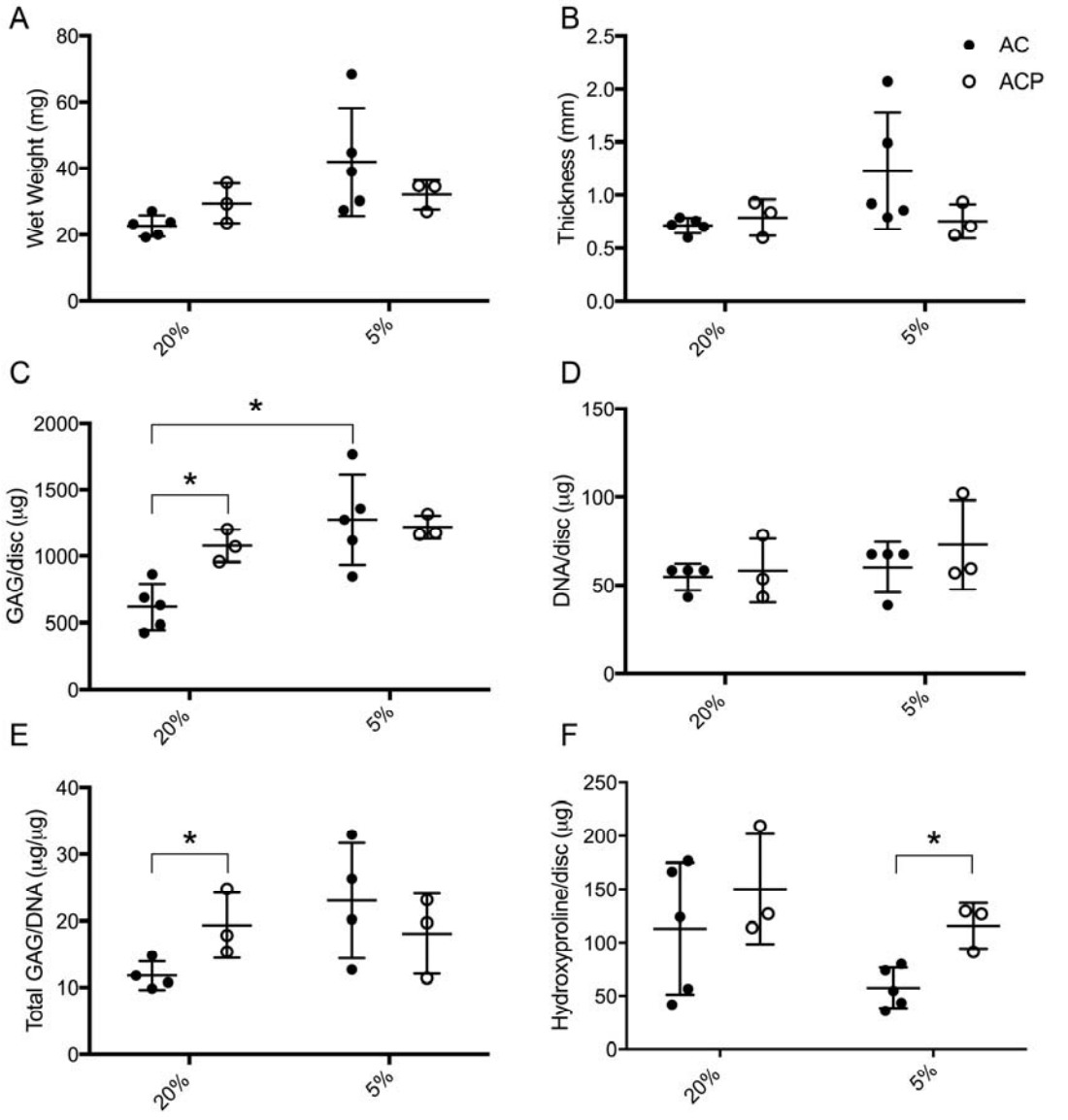

Figure 3. (A) Tissue wet weight and (B) thickness were not different between cell type or oxygen level. Quantitative measurements for biochemical constituents of the neocartilage discs including (C,E) glycosaminoglycans (GAGs) as a readout for total proteoglycan content, (D) DNA for relative cell count, and (F) hydroxyproline for total collagen content indicate that relative to hyperoxia, culture in physioxia significantly increased total GAG content for only ACs. ACPs, however, had a significantly higher total collagen content in than ACs culture in physioxia. Results reported as mean + SD, and statistical significance was determined as *$p<0.05$ by a paired or unpaired t-test where appropriate.

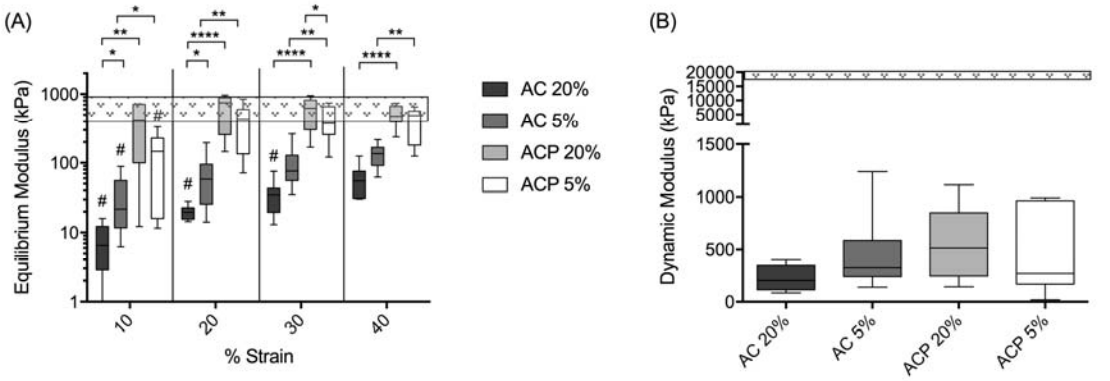

Figure 4. Quantitative analysis of (A) equilibrium compressive modulus reveals that scaffold-free neocartilage demonstrated strain stiffening behavior, physioxia significantly increased the bulk compressive equilibrium modulus for AC neocartilage, and ACP neocartilage was significantly stronger than AC neocartilage. There were no differences in (B) dynamic compressive modulus between cell types or oxygen levels. Results reported as a box plot representing mean, the 1st and 3rd quartiles, and SD. Statistical significance was determined as *p<0.05, **p<0.01, ****p<0.0001 by a paired t-test within a cell type between oxygen levels, an unpaired t-test between cell types within a given oxygen level. Statistical significance between consecutive strain ramps for a given group was determined as #p<0.05 to characterize strain stiffening. Chevron box represents range of reported values for native adult articular cartilage (45,54,55).

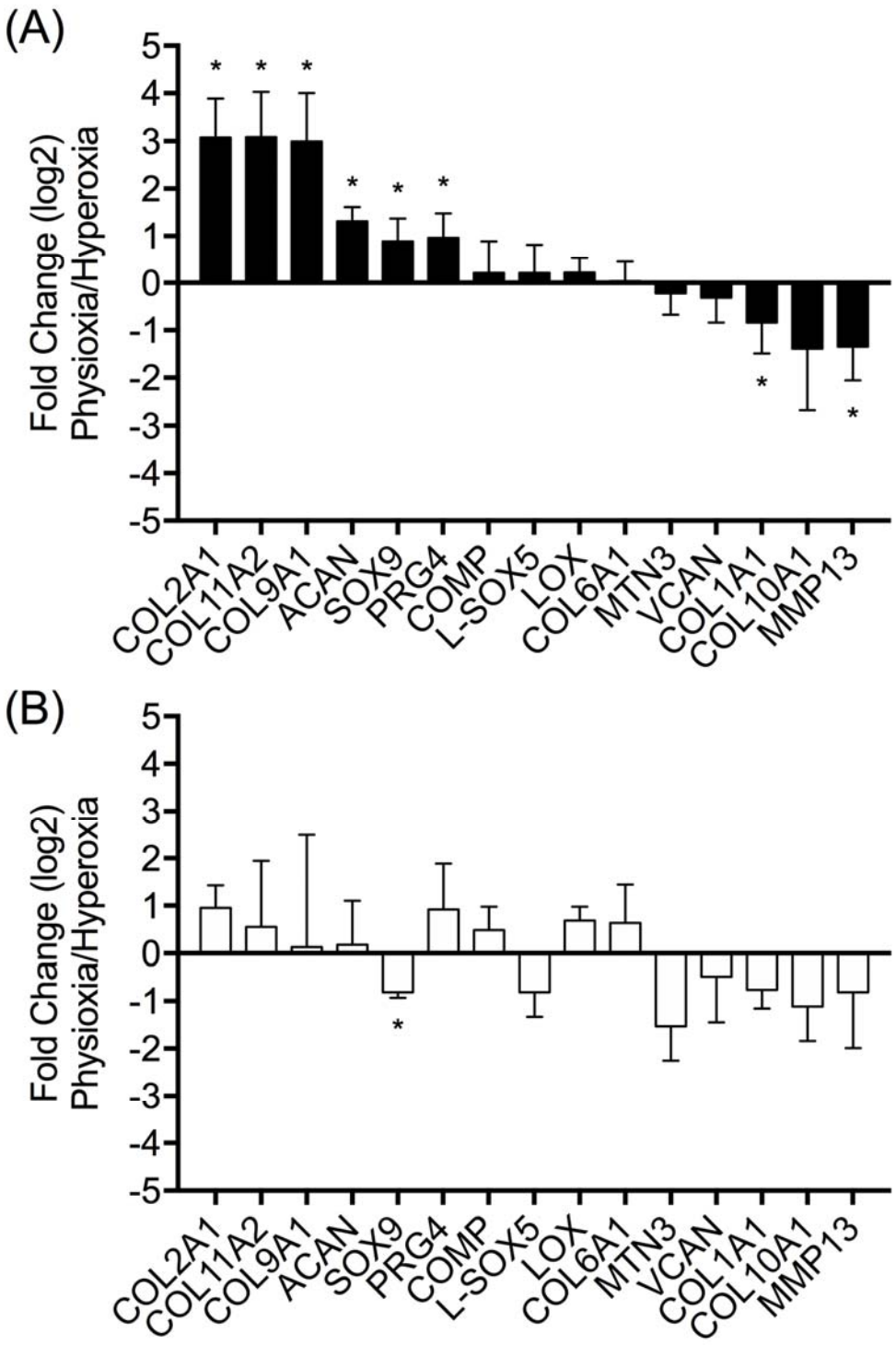

Figure 5. Fold change in chondrogenic gene expression for culture in physioxia relative to hyperoxia demonstrates that (A) ACs, but not (B) ACPs, were highly responsive to oxygen level and upregulated genes representative of the articular cartilage phenotype in

physioxia. Results reported as mean ± SD of log2 fold change, and statistical significance for comparison of mean expression in physioxia versus hyperoxia was determined as *p<0.05 by a paired or unpaired t-test where appropriate.

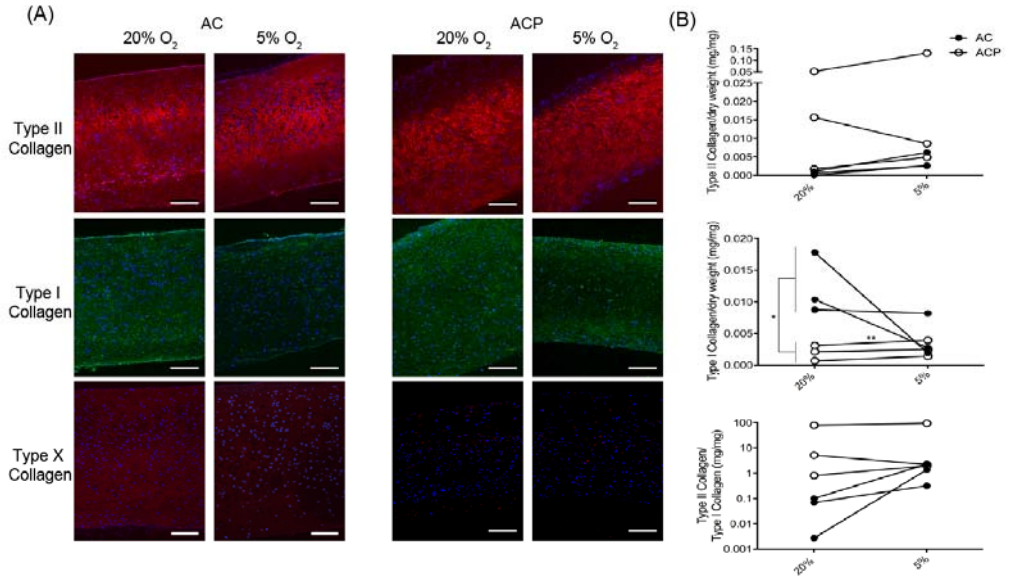

Figure 6. (A) Collagen immunohistochemistry demonstrates consistently high type II collagen expression in tissues derived from both ACs and ACPs in hyperoxia and physioxia but reduced type I collagen for both AC- and ACP-derived tissues in physioxia relative to hyperoxia. AC-derived neocartilage had low type X collagen expression in hyperoxia that was undetectable in physioxia, but ACP-derived neocartilage lacked type X collagen at both oxygen levels. (B) Quantification of collagen by ELISA indicates that ACP-derived neocartilage contained more type II than type I collagen regardless of oxygen level, but AC-derived neocartilage increases the ratio of type II to I collagen with culture in physioxia relative to hyperoxia. Scale bars = 100 μm.

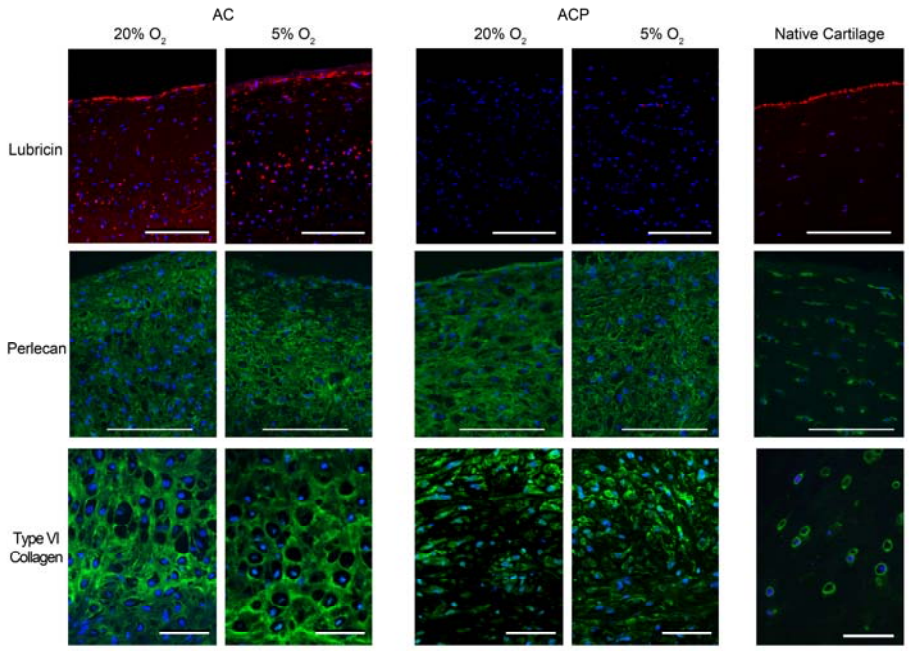

Figure 7. Immunohistochemistry of lubricin, perlecan, and type VI collagen revealed that only AC-derived neocartilage produced lubricin that was localized to the surface regardless of oxygen level. Also independent of oxygen level, neocartilage from both cell types produced perlecan that was distributed throughout the extracellular matrix, and ACP-derived neocartilage had type VI collagen localized to the pericellular matrix while type VI collagen was distributed throughout the entire extracellular matrix for AC-derived neocartilage. Scale bars = 100 μm for lubricin and perlecan, 20 μm for type VI collagen.

Tissue Engineering
Physioxia promotes the articular chondrocyte-like phenotype in human chondroprogenitor-derived self-organized tissue
 (DOI: 10.1089/ten.TEA.2016.0510)
This paper has been peer-reviewed and accepted for publication, but has yet to undergo copyediting and proof correction. The final published version may differ from this proof.

Table S1. TaqMan Primers

Gene	TaqMan Primer
ACAN	Hs00153936_m1
COL1A1	Hs00164004_m1
COL2A1	Hs00264051_m1
COL6A1	Hs00242448_m1
COL9A1	Hs00932129_m1
COL10A1	Hs00166657_m1
COL11A2	Hs00365416_m1
COMP	Hs00164359_m1
LOX	Hs00942480_m1
MMP13	Hs00233992_m1
MTN3	Hs00159081_m1
PRG4	Hs00195140_m1
L-SOX5	Hs00374709_m1
SOX9	Hs01001343_g1
TBP	Hs00427620_m1
VCAN	Hs00171642_m1